

# Many-to-Many Matching via Sparsity Controlled Optimal Transport

Weijie Liu, Han Bao, Makoto Yamada, Zenan Huang, Nenggan Zheng, *Senior Member, IEEE*, Hui Qian

**Abstract**—Many-to-many matching seeks to match multiple points in one set and multiple points in another set, which is a basis for a wide range of data mining problems. It can be naturally recast in the framework of Optimal Transport (OT). However, existing OT methods either lack the ability to accomplish many-to-many matching or necessitate careful tuning of a regularization parameter to achieve satisfactory results. This paper proposes a novel many-to-many matching method to explicitly encode many-to-many constraints while preventing the degeneration into one-to-one matching. The proposed method consists of the following two components. The first component is the matching budget constraints on each row and column of a transport plan, which specify how many points can be matched to a point at most. The second component is the deformed  $q$ -entropy regularization, which encourages a point to meet the matching budget maximally. While the deformed  $q$ -entropy was initially proposed to sparsify a transport plan, we employ it to avoid the degeneration into one-to-one matching. We optimize the objective via a penalty algorithm, which is efficient and theoretically guaranteed to converge. Experimental results on various tasks demonstrate that the proposed method achieves good performance by gleaning meaningful many-to-many matchings.

**Index Terms**—many-to-many matching, optimal transport

## I. INTRODUCTION

**M**ATCHING two related sets is a fundamental problem in data mining [1]–[3]. Real-world applications may require matching each point in one set to multiple points in

Manuscript received April 19, 2021; revised August 16, 2021. (*Corresponding author: Nenggan Zheng.*)

This work is supported by National Key Research and Development Program of China under Grant 2020AAA0107400, Major Program of the National Natural Science Foundation of China (T2293723), and National Natural Science Foundation of China (Grant No: 62206248).

Weijie Liu is with the Qiushi Academy for Advanced Studies, Zhejiang University, Hangzhou, Zhejiang 310007, China, and also with the College of Computer Science and Technology, Zhejiang University, Hangzhou, Zhejiang 310007, China (e-mail: westonhunter.zju.edu.cn).

Han Bao is with Kyoto University, Yoshidahonmachi, Sakyo Ward, Kyoto, 606-8501, Japan (e-mail: bao@i.kyoto-u.ac.jp).

Makoto Yamada is with Okinawa Institute of Science and Technology, Kunigami-gun, Okinawa 904-0497, Japan, and also with RIKEN Center for Advanced Intelligence Project, Chuo-ku, Tokyo 103-0027, Japan (e-mail: makoto.yamada@oist.jp).

Zenan Huang is with the College of Computer Science and Technology, Zhejiang University, Hangzhou, Zhejiang 310007, China (e-mail: lccurious@zju.edu.cn).

Nenggan Zheng is with the Qiushi Academy for Advanced Studies, Zhejiang University, Hangzhou, Zhejiang 310007, China, and also with the Collaborative Innovation Center for Artificial Intelligence by MOE and Zhejiang Provincial Government (ZJU) and the Zhejiang Laboratory, Hangzhou, Zhejiang 311121, China (e-mail: zng@cs.zju.edu.cn).

Hui Qian is with the College of Computer Science and Technology, Zhejiang University, Hangzhou, Zhejiang 310007, China, and also with State Key Lab of CAD&CG, Zhejiang University, Hangzhou, Zhejiang 310007, China (e-mail: qianhui@zju.edu.cn).

another set, that is, many-to-many matching [4]–[6]. Such applications include information retrieval [7], point cloud registration [8], associating proteins across species [9], and recommendation systems [10]. In these applications, many-to-many matching shall be considered because no strict one-to-one correspondence exists in the data (refer to Figure 1 for an illustration), or users desire more recommended items [10]. Mathematically speaking, many-to-many matching is formulated as finding a matching matrix by optimizing the overall utility while satisfying matching budget constraints, that is, the number of non-zero entries in each row and each column are upper-bounded. Such a problem can be naturally rephrased in the powerful and elegant framework of Optimal Transport (OT) [11].

Dating back to [12], OT compares two probability distributions by finding a transport plan between them that minimizes the overall cost [11], [13]. In the past decade, OT has been employed to address a broad class of problems, including ranking [14], [15], graph mining [16], [17], and cross-domain retrieval [18], [19], among others. The majority of research in this area focuses on calculating the Wasserstein distance [20] or identifying a transport plan that establishes correspondence between two datasets [13].

While it is possible to establish many-to-many matching by selecting relatively large entries in a transport plan, the lack of a principled formulation eventually leads to brittle solutions. A group of works attempts to simply model many-to-many matching as OT by considering points with non-zero entries in a transport plan as matched pairs [21]–[24]. This post-process often results in a matching matrix with very few points being matched because solutions to the vanilla OT are usually too sparse [25], [26]. The entropy regularization has been commonly used to prevent a transport plan from being overly sparse and enhance numerical stability [27], which results in a fuzzy transport plan and renders it difficult to extract an interpretable matching [28]–[31]. Therefore, it is crucial to maintain a transport plan that satisfies the matching budget while avoiding the degeneration into one-to-one matching by controlling the sparsity.

To effectively and efficiently conduct many-to-many matching, this paper proposes a new method, Sparsity Controlled Optimal Transport for Many-to-many matching (SCOTM), which consists of two components. First, to enforce the matching budget, we impose the sparsity constraints on both the rows and columns of a transport plan. Second, to prevent a transport plan from being overly sparse, we regularize the transport plan with the deformed  $q$ -entropy that was initially proposed to sparsify a transport plan [30]. SCOTM encourages

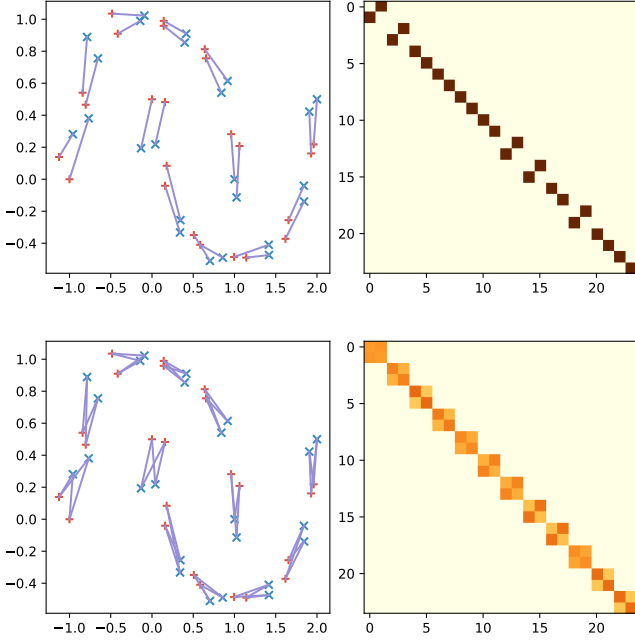


Fig. 1: The matching results (left) and the transport plans (right) between two uniform discrete measures obtained by the network simplex solver for OT (top) and our method (bottom), respectively. The red +’s and the blue ×’s denote the support points of the two measures, respectively. The darker the color is, the larger the value of the corresponding entry in the transport plan is. Since the support points do not have strict one-to-one correspondence, many-to-many matching is more appropriate.

as many points to be matched as possible under the matching budget by adjusting the value of  $q$ . This novel application of the deformed  $q$ -entropy is of independent interest. We then propose a penalty algorithm to decompose the intricate feasible domain into the intersection of four sets, each of which admits a closed-form update of the projection step. Our contributions can be summarized as follows:

- 1) We introduce a practical OT-based many-to-many matching formulation, which imposes the row/column sparsity constraints and promotes matches using the  $q$ -entropy regularization.
- 2) We develop an efficient penalty algorithm to handle the complex feasible domain and solve the underlying optimization problem of SCOTM.
- 3) We prove that the sequence of the transport plan output by the penalty algorithm admits a limit point, which satisfies the first-order optimality condition.

Empirical results in a variety of tasks demonstrate that SCOTM outperforms state-of-the-art methods. Specifically, synthetic experiments illustrate that SCOTM can control the transport plan sparsity more flexibly than existing OT variants. Experiments in student course allocation, matching protein interaction networks, and object recognition show that SCOTM performs well in a wide range of real-world applications.

The rest of the paper is organized as follows. In the next

section, a comprehensive review of the background is given. Section III delineates the proposed many-to-many matching method. Experimental results on various tasks are reported in Section IV. The appendix provides detailed theoretical proofs.

## II. PRELIMINARY AND RELATED WORK

### A. Notation

For  $x \in \mathbb{R}$ , let  $[x]_+ = x$  if  $x > 0$  and 0 otherwise. We use bold lowercase symbols (e.g.  $\mathbf{x}$ ), bold uppercase letters (e.g.  $\mathbf{X}$ ), uppercase calligraphic fonts (e.g.  $\mathcal{X}$ ), and Greek letters (e.g.  $\alpha$ ) to denote vectors, matrices, spaces (sets), and measures, respectively. The  $d$ -dimensional all-ones vector is denoted by  $\mathbf{1}^d \in \mathbb{R}^d$ . The probability simplex with  $d$  bins is denoted by  $\Delta^d$ , namely  $\Delta^d = \{\mathbf{a} \in \mathbb{R}_+^d \mid \sum_{i=1}^d a_i = 1\}$ . The expression  $\mathbf{x} \geq c$  (resp.  $\mathbf{X} \geq c$ ) indicates that each entry of the vector  $\mathbf{x}$  (resp. the matrix  $\mathbf{X}$ ) is greater than or equal to the scalar  $c$ . In the matrix  $\mathbf{X}$ ,  $\mathbf{X}[i, :]$  represents the  $i^{\text{th}}$  row, and  $\mathbf{X}[:, j]$  denotes the  $j^{\text{th}}$  column. Given a matrix  $\mathbf{X}$ , expressions  $\|\mathbf{X}\|_F$ ,  $\|\mathbf{X}\|_0$ , and  $\|\mathbf{X}\|_\infty$  denote its Frobenius norm, number of non-zero elements, and maximum absolute value (i.e.,  $\|\mathbf{X}\|_\infty = \max_{i,j} |X_{ij}|$ ), respectively. The cardinality of set  $\mathcal{X}$  is denoted by  $|\mathcal{X}|$ . The bracketed notation  $\llbracket n \rrbracket$  is the shorthand for the integer set  $\{1, 2, \dots, n\}$ . A discrete measure  $\alpha$  is denoted by  $\alpha = \sum_{i=1}^m a_i \delta_{\mathbf{x}_i}$ , where  $\delta_{\mathbf{x}}$  is the Dirac measure at position  $\mathbf{x}$ , i.e., a unit of mass infinitely concentrated at  $\mathbf{x}$ . When  $\alpha$  is a probability measure,  $\mathbf{a} = [a_i]$  is in the simplex  $\mathbf{a} \in \Delta^m$ .

### B. Many-to-many Matching

Over the past few decades, many-to-many matching has received a lot of attention in numerous fields including combinatorial optimization [32], [33], operations research [34]–[36], and economics [37]–[39]. Given two disjoint sets  $\mathcal{S} = \{s_1, s_2, \dots, s_m\}$  and  $\mathcal{T} = \{t_1, t_2, \dots, t_n\}$ , many-to-many matching involves finding a binary matching matrix  $\mathbf{T} = [T_{ii'}] \in \{0, 1\}^{m \times n} \cap \Omega_{\rho^s, \rho^t}$  between  $\mathcal{S}$  and  $\mathcal{T}$  satisfying prescribed budget constraints denoted by  $\Omega_{\rho^s, \rho^t}$ , i.e.,  $T_{ii'} = 1$  if  $s_i$  is matched to  $t_{i'}$  and  $T_{ii'} = 0$  otherwise, and  $\mathbf{T} \in \Omega_{\rho^s, \rho^t}$  indicates that  $\mathbf{T}$  has at most  $\rho^s$  and  $\rho^t$  non-zero entries in each row and column, respectively:

$$\Omega_{\rho^s, \rho^t} = \left\{ \mathbf{T} \in \mathbb{R}_+^{m \times n} \mid \|\mathbf{T}[i, :]\|_0 \leq \rho^s \text{ for all } i, \right. \\ \left. \text{and } \|\mathbf{T}[:, i']\|_0 \leq \rho^t \text{ for all } i' \right\}.$$

Typical examples of many-to-many matching include the following scenarios:

- 1) Curriculum management system: Each student (from set  $\mathcal{S}$ ) has a limit  $\rho^s$  on the number of courses he or she can attend, while each course (from set  $\mathcal{T}$ ) has a limit  $\rho^t$  on the number of students that it can admit [40], [41]. This scenario represents a combinatorial optimization challenge within an educational context, where the goal is to optimally allocate courses to students based on their preferences and course capacities.
- 2) Matching Protein Interaction Networks (PINs): Proteins and their interactions are at the core of almost every

biological process. In a PIN, nodes represent proteins and edges correspond to interactions between proteins. By matching PINs across different species, it is possible to establish correspondences between proteins, thereby performing protein function predictions and transferring protein knowledge from well-studied species like mice to other species [42].

- 3) Task assignment: Project management systems are ubiquitous in various organizations where tasks and agents are represented as two distinct sets. One task can be assigned to multiple agents, and conversely, an agent may undertake multiple tasks [32], [33]. A many-to-many matching method can be used to efficiently assign tasks to agents, considering constraints like the capability of agents and the requirements of each task.
- 4) Video caching: In a bandwidth-constrained network, base stations select videos to cache according to their local popularity to reduce end-users' experienced delay [34]. Each video can be cached by multiple base stations and each base station can cache multiple videos, which allows the video caching system to better balance the load on the network and improve the overall user experience.

Existing non-OT many-to-many matching methods primarily fall into the following two categories.

**Multi-objective optimization.** Some methods formulate many-to-many matching as multi-objective optimization problems [38], [40], [43]–[45]. By modeling each point as an autonomous agent that has a preference ranking over points from the other set, these methods match each point to as high-ranking points as possible while achieving Pareto optimality and stability. Nevertheless, these methods usually have high computational complexities because each iteration requires finding a Pareto improvement, which involves  $\mathcal{O}(m^2n^2)$  time [38], [43].

**Single-objective optimization.** Several studies formulated many-to-many matching based on single objective optimization by encoding the preferences with a preference matrix  $\mathbf{R} = [R_{ii'}]$ , as follows [4], [5], [46]:

$$\max_{\mathbf{T} \in \{0,1\}^{m \times n} \cap \Omega_{\rho^s, \rho^t}} \sum_{i=1}^m \sum_{i'=1}^n R_{ii'} T_{ii'}. \quad (1)$$

To solve the problem (1), it has been common to use the Hungarian method [32], [46], [47] or solve its continuous relaxation with the interior point method [33]. These approaches have computational complexity  $\mathcal{O}(\max\{m, n\}^3 \max\{\rho^s, \rho^t\}^3)$ , which is more efficient than multi-objective optimization methods when  $m$  and  $n$  are of the same order, and both  $\rho^s$  and  $\rho^t$  are relatively small. However, when  $\rho^s$  or  $\rho^t$  is large, they can also be time-consuming. In addition, a naive solution to the problem (1) may be *excessively sparse* such that each point matches to only a very small number of points. Even if such a solution is feasible for (1), we desire to obtain a solution that matches as many points as possible under the budget constraints.

Another limitation of these non-OT methods is that they treat all points in  $\mathcal{S}$  (resp.  $\mathcal{T}$ ) with equal importance. In some situations, we may need to prioritize matching certain

points. For example, in task assignment, some tasks may be more urgent or important, necessitating prioritized resource allocation. Though this might be achievable in single-objective optimization methods by modifying the preference matrix in an ad-hoc manner, such modifications typically demand careful control. This limitation can be naturally and effectively addressed by our OT-based many-to-many matching method that is derived in Section III. We first review OT in the following subsection.

### C. Optimal Transport and Its Variants

**Optimal Transport.** Given discrete probability measures  $\alpha = \sum_{i=1}^m a_i \delta_{\mathbf{x}_i}$  and  $\beta = \sum_{i'=1}^n b_{i'} \delta_{\mathbf{y}_{i'}}$ , OT is formulated by the following optimization problem:

$$\min_{\mathbf{T} \in \Pi(\mathbf{a}, \mathbf{b})} \left\{ \ell(\mathbf{T}) := \sum_{i=1}^m \sum_{i'=1}^n c(\mathbf{x}_i, \mathbf{y}_{i'}) T_{ii'} \right\}, \quad (2)$$

where  $c(\cdot, \cdot)$  is a cost function and the feasible domain of *transport plan*  $\mathbf{T} = [T_{ii'}]$  is given by the set

$$\Pi(\mathbf{a}, \mathbf{b}) = \{ \mathbf{T} \in \mathbb{R}_+^{m \times n} \mid \mathbf{T} \mathbf{1}^n = \mathbf{a}, \mathbf{T}^\top \mathbf{1}^m = \mathbf{b} \}.$$

The optimal objective value of (2) is often referred to as the OT distance [11], [26]. The problem (2) is a linear program and can be solved by off-the-shelf linear programming methods [48], [49] which, however, incur cubic computational complexities and are not scalable to large datasets.

**Entropy regularized OT.** To enhance the scalability, [27] proposed to regularize a transport plan with the negative Shannon entropy as follows:

$$\min_{\mathbf{T} \in \Pi(\mathbf{a}, \mathbf{b})} \ell(\mathbf{T}) - \gamma H(\mathbf{T}),$$

where  $\gamma > 0$  is the regularization weight and  $H(\mathbf{T}) = -\sum_{i=1}^m \sum_{i'=1}^n (T_{ii'} \log T_{ii'} - T_{ii'})$  is the negative Shannon entropy. [27] showed that the regularized problem can be solved by the Sinkhorn algorithm, whose computational complexity is quadratic. However, the resulting transport plan is strictly positive and completely dense, which is undesirable in many applications where a transport plan is of interest [28], [29].

**Quadratic regularized OT.** [28] instead considered the quadratic regularization as follows:

$$\min_{\mathbf{T} \in \Pi(\mathbf{a}, \mathbf{b})} \ell(\mathbf{T}) + \gamma \sum_{i'=1}^n \left\| \mathbf{T}[:, i'] \right\|_2^2.$$

It is shown that the quadratic regularization can induce sparsity in the resulting transport plan.

**$q$ -regularized OT.** [30] further introduced the *deformed  $q$ -entropy*, which is defined as follows:

$$H_q(\mathbf{T}) = \begin{cases} \frac{-1}{2-q} \sum_{i=1}^m \sum_{i'=1}^n \left( \frac{T_{ii'}^{2-q} - T_{ii'}}{1-q} - T_{ii'} \right), & \text{if } q \in [0, 1), \\ -\sum_{i=1}^m \sum_{i'=1}^n (T_{ii'} \log T_{ii'} - T_{ii'}), & \text{if } q = 1. \end{cases}$$

The deformed  $q$ -entropy requires  $q \in [0, 1]$  and recovers the negative Shannon entropy and quadratic regularization at  $q = 1$  and  $q = 0$ , respectively. As  $q$  approaches 1, the solution becomes less sparse, and it becomes completely dense if  $q = 0$ . Therefore, by using the deformed  $q$ -entropy as

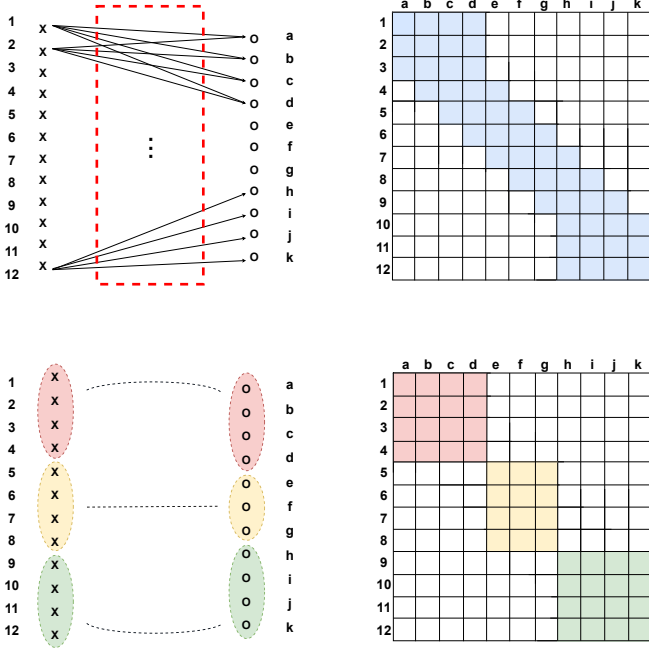


Fig. 2: A comparison between many-to-many matching (top) and cluster-to-cluster matching (bottom) in the student course allocation problem. The sets of students and courses are denoted as  $\{1, 2, \dots, 12\}$  and  $\{a, b, \dots, k\}$ , respectively. Each student can take up to 4 courses and each course can admit up to 6 students. In the cluster-to-cluster matching, the students are divided into the three clusters (groups), and all students in each cluster take exactly the same courses.

regularization, the sparsity of a transport plan can be controlled by varying the parameter  $q$ , as follows:

$$\min_{\mathbf{T} \in \Pi(\mathbf{a}, \mathbf{b})} \ell(\mathbf{T}) - \gamma H_q(\mathbf{T}).$$

In this work, we heavily leverage the sparsity control with the deformed  $q$ -entropy to obtain a transport plan that maximally satisfies the row/column budget constraints of many-to-many matching.

**Sparsity-constrained OT.** [31] applied explicit cardinality constraints on the columns of a transport plan as follows:

$$\min_{\mathbf{T} \in \Pi(\mathbf{a}, \mathbf{b})} \ell(\mathbf{T}) + \gamma \sum_{i'=1}^n \|\mathbf{T}[:, i']\|_2^2, \text{ s.t. } \forall i', \|\mathbf{T}[:, i']\|_0 \leq \rho.$$

Such a formulation enables direct control of the sparsity of each column in a transport plan. However, it cannot be directly used for many-to-many matching, because (i) there is no cardinality constraint applied in the row direction, which may result in too many non-zero entries in some rows, and (ii) the resulting transport plan is likely to be overly sparse, which leads to nearly one-to-one matching.

#### D. Further Related Work

**Cluster-to-cluster matching.** A closely related problem is cluster-to-cluster matching [50]–[53], which requires simultaneous assignment of each point to a cluster and determination

of the one-to-one correspondence between clusters.<sup>1</sup> If a cluster  $\mathcal{I} \subset \mathcal{S}$  is matched to a cluster  $\mathcal{I}' \subset \mathcal{T}$ , all points in the cluster  $\mathcal{I}$  are matched to the cluster  $\mathcal{I}'$ , and the specific points matching within the clusters are not of concern. A cluster-to-cluster matching can also be decomposed into two separate many-to-one matches, that is, matching the two sets to a virtual set [50]. The feasible domain of cluster-to-cluster matching is a subset of the feasible domain of many-to-many matching when the cardinalities of sets  $\mathcal{I}$  and  $\mathcal{I}'$  are constrained by  $|\mathcal{I}| \leq \rho^t$  and  $|\mathcal{I}'| \leq \rho^s$  respectively, which demonstrates that many-to-many matching can accommodate more flexible matching structures. See Figure 2 for an illustration in the context of a student-course allocation problem. In addition, some clusters may contain a single point, which results in one-to-one or many-to-one matching for these points.

**OT-based one-to-one matching.** Many works in the OT literature involve obtaining one-to-one matching from the calculated transport plan [16], [17], [54]. To this end, they solve a linear assignment problem based on the transport plan, or simply choose the largest entry in each row (or column) of the transport plan to indicate the matching. One-to-one matching methods are characterized by matching matrices with at most one non-zero entry per row and column, which is a special case of many-to-many matching when  $\rho^s = 1$  and  $\rho^t = 1$ . Some works further seek to incorporate structures of probability distributions into a transport plan [55]–[57]. Closely related to our work, [55] proposed to encourage correlations in matchings of source supports that are close, which however does not control the sparsity of a transport plan explicitly.

### III. METHODOLOGY

In this section, we first present our OT-based many-to-many matching formulation. Then, an optimization algorithm is derived. We finally demonstrate the convergence guarantee of the proposed algorithm. For conciseness, all detailed proofs are deferred to the appendix.

#### A. Problem Formulation

First, we recast many-to-many matching into the following OT problem with the additional budget constraints:

$$\min_{\mathbf{T}} \ell(\mathbf{T}), \text{ s.t. } \mathbf{T} \in \Pi(\mathbf{a}, \mathbf{b}) \cap \Omega_{\rho^s, \rho^t}, \quad (3)$$

which, as is implied by the following theorem, is well-defined under suitable assumptions.

**Theorem III.1.** *Let  $\mathcal{J}'(h)$  (resp.  $\mathcal{J}(h)$ ) be a subset of  $\llbracket n \rrbracket$  (resp.  $\llbracket m \rrbracket$ ) with cardinality  $h$ . When the following conditions hold:*

$$\|\mathbf{a}\|_\infty \leq \min_{\mathcal{J}'(\rho^s-1) \subset \llbracket n \rrbracket} \sum_{i' \in \mathcal{J}'(\rho^s-1)} b_{i'}, \quad (4)$$

and

$$\|\mathbf{b}\|_\infty \leq \min_{\mathcal{J}(\rho^t-1) \subset \llbracket m \rrbracket} \sum_{i \in \mathcal{J}(\rho^t-1)} a_i, \quad (5)$$

<sup>1</sup>Although some of these works also use the terminology “many-to-many matching”, this paper refers to this type of matching as cluster-to-cluster matching to distinguish the two notions.

the feasible domain  $\Pi(\mathbf{a}, \mathbf{b}) \cap \Omega_{\rho^s, \rho^t}$  is non-empty.

Therefore, (3) can be regarded as a well-defined continuous alternative of (1) when  $\rho^s$  and  $\rho^t$  satisfy (4) and (5), making it possible to solve many-to-many matching problems more efficiently. By the Extreme Value Theorem [58], the continuous objective function over the non-empty and compact feasible domain  $\Pi(\mathbf{a}, \mathbf{b}) \cap \Omega_{\rho^s, \rho^t}$  has a minimum. Once a solver for (3) outputs a transport plan, many-to-many matching can simply be indicated by its non-zero entries. Another advantage of (3) over (1) is that it can set non-uniform distributions  $\mathbf{a}$  and/or  $\mathbf{b}$  to prioritize some points, as is formalized in the following theorem.

**Theorem III.2.** Assume that  $\mathbf{a}$  and  $\mathbf{b}$  satisfy (4) and (5). When

$$a_i \geq \max_{\mathcal{J}'(h) \subset \llbracket n \rrbracket} \sum_{i' \in \mathcal{J}'(h)} b_{i'}, \quad (6)$$

where  $h \in \llbracket \rho^s - 1 \rrbracket$ , at least  $h$  points are matched to  $s_i$ . Similarly, when

$$b_{i'} \geq \max_{\mathcal{J}(h) \subset \llbracket m \rrbracket} \sum_{i \in \mathcal{J}(h)} a_i, \quad (7)$$

where  $h \in \llbracket \rho^t - 1 \rrbracket$ , at least  $h$  points are matched to  $t_{i'}$ .

Theorem III.2 implies that our formulation can ensure a flexible lower bound  $h$  of the number of points matched to a prioritized point. More specifically, the design of  $\mathbf{a}$  and  $\mathbf{b}$  has to firstly satisfy the conditions in Theorem III.1 to ensure that the feasible domain is non-empty. Secondly,  $\mathbf{a}$  (resp.  $\mathbf{b}$ ) needs to satisfy Eq. (6) (resp. (7)) to guarantee that at least  $h$  points are matched to prioritized points in  $\mathcal{S}$  (resp.  $\mathcal{T}$ ), which is demonstrated in the following example.

**Example III.3.** Without loss of generality, the proportion of prioritized points in  $\mathcal{S}$  is denoted by  $r$ , and assume that at least  $h$  points need to be matched to prioritized points. Then,  $\mathbf{b}$  can still be set as a uniform distribution while  $\mathbf{a} = [a_i]$  can be chosen as follows:

$$a_i = \begin{cases} \frac{h}{n}, & \text{if } i \text{ is a prioritized point,} \\ \frac{1-mrh/n}{m-mr}, & \text{otherwise,} \end{cases} \quad (8)$$

where  $h \in \llbracket \rho^s - 1 \rrbracket$ . It is obvious that  $\sum_{i=1}^m a_i = 1$ . Under such a setting, as long as  $m$ ,  $n$ , and  $h$  satisfy

$$n \leq mh, \quad (9)$$

(4), (5) and (6) hold simultaneously. Note that Eq. (7) is not required to hold since only some points in  $\mathcal{S}$  are prioritized.

**Deformed  $q$ -entropy regularization.** One limitation of the formulation (3) is that the budget constraints entail only the upper bounds of the row/column cardinalities, and thus even a feasible solution can be so sparse that it degenerates into nearly one-to-one matching. Hence, an additional technique is needed to encourage matching as many points as possible. We propose to adopt the deformed  $q$ -entropy regularization to address this issue by considering the following regularized problem:

$$\min_{\mathbf{T} \in \Pi(\mathbf{a}, \mathbf{b}) \cap \Omega_{\rho^s, \rho^t}} \left\{ G(\mathbf{T}) := \ell(\mathbf{T}) - \gamma H_q(\mathbf{T}) \right\}, \quad (10)$$

---

**Algorithm 1** Penalty Algorithm for the problem (10).

---

- 1: **Input:** Initialized variables  $\mathbf{T}^{(0)} = \mathbf{U}^{(0)} = \mathbf{V}^{(0)} = \mathbf{W}^{(0)}$  s.t.  $\mathbf{T}^{(0)} \in \Pi(\mathbf{a}, \mathbf{b}) \cap \Omega_{\rho^s, \rho^t}$ , scalars  $\sigma^{(0)} > 0$  and  $\theta > 1$ , and a sequence  $\{\epsilon^{(k)}\}_k$  s.t.  $\epsilon^{(k)} \rightarrow 0$ .
- 2: **Output:** The sequence  $\{\mathbf{T}^{(k)}\}$ .
- 3: **for**  $k = 0, 1, \dots$  **do**
- 4: Calculate the element-wise partial gradient of  $J_{\sigma^{(k)}}(\cdot)$  w.r.t.  $\mathbf{T}^{(k)}$ :

$$\mathbf{D}^{(k)} = \frac{\partial J_{\sigma^{(k)}}(\mathbf{T}^{(k)}, \mathbf{U}^{(k)}, \mathbf{V}^{(k)}, \mathbf{W}^{(k)})}{\partial \mathbf{T}},$$

and find step-size  $\eta$  via the Armijo line search in the direction  $-\mathbf{D}^{(k)}$ .

- 5: Calculate  $\mathbf{T}_{\text{trial}} = \text{proj}_{\Omega^1}(\mathbf{T}^{(k)} - \eta \mathbf{D}^{(k)})$ .
  - 6: **if**  $J_{\sigma^{(k)}}(\mathbf{T}_{\text{trial}}, \mathbf{U}^{(k)}, \mathbf{V}^{(k)}, \mathbf{W}^{(k)}) \leq G(\mathbf{T}^{(0)})$  **then**
  - 7:     **Set**  $\mathbf{T}^{(k,0)} = \mathbf{T}^{(k)}$ ,  $\mathbf{U}^{(k,0)} = \mathbf{U}^{(k)}$ ,  $\mathbf{V}^{(k,0)} = \mathbf{V}^{(k)}$ , and  $\mathbf{W}^{(k,0)} = \mathbf{W}^{(k)}$ .
  - 8:     **else**
  - 9:         **Set**  $\mathbf{T}^{(k,0)} = \mathbf{T}^{(0)}$ ,  $\mathbf{U}^{(k,0)} = \mathbf{U}^{(0)}$ ,  $\mathbf{V}^{(k,0)} = \mathbf{V}^{(0)}$ , and  $\mathbf{W}^{(k,0)} = \mathbf{W}^{(0)}$ .
  - 10:     **end if**
  - 11:     **Set**  $l = 0$ .
  - 12:     **while**  $\|\mathbf{T}^{(k,l+1)} - \mathbf{T}^{(k,l)}\|_F > \epsilon^{(k)}$  **do**
  - 13:         Find step-size  $\eta$  via the Armijo line search in the direction  $-\mathbf{D}^{(k,l)}$ .
  - 14:         Calculate  $\mathbf{T}^{(k,l+1)}$  as Eq. (12).
  - 15:         Calculate  $\mathbf{U}^{(k,l+1)}$ ,  $\mathbf{V}^{(k,l+1)}$ , and  $\mathbf{W}^{(k,l+1)}$  independently as Eq. (13).
  - 16:         Update  $l = l + 1$ .
  - 17:     **end while**
  - 18:     **Set**  $\sigma^{(k+1)} = \theta \sigma^{(k)}$ .
  - 19:     **Set**  $\mathbf{T}^{(k+1)} = \mathbf{T}^{(k,l)}$ ,  $\mathbf{U}^{(k+1)} = \mathbf{U}^{(k,l)}$ ,  $\mathbf{V}^{(k+1)} = \mathbf{V}^{(k,l)}$ , and  $\mathbf{W}^{(k+1)} = \mathbf{W}^{(k,l)}$ .
  - 20: **end for**
- 

where a value close to 1 should be chosen for  $q$  to induce as dense a solution as possible under the budget constraints. Our formulation achieves many-to-many matching by controlling the sparsity of transport plans, and is thus referred to as Sparsity Controlled Optimal Transport for Many-to-many matching (SCOTM). It is worth noting that the common negative Shannon entropy is inapplicable, because the gradients of the regularized objective with respect to a transport plan are ill-defined in the feasible region of the problem (10).

**Remark.** Problem (10) involves a convex optimization objective and a non-convex feasible domain. One may wonder whether it is possible to relax (10) by discarding the non-convex  $\Omega_{\rho^s, \rho^t}$  and using a convex sparsity-inducing regularizer (e.g., the  $\ell_1$  norm). Unfortunately, such an approach does not grant us direct control over the number of non-zero entries in each row and column. Moreover, adding the  $\ell_1$  norm regularizer of a transport plan is ineffective, because it is equivalent to adding a constant to the objective and does not influence the solution, that is,

$$\min_{\mathbf{T} \in \Pi(\mathbf{a}, \mathbf{b})} G(\mathbf{T}) + \lambda \|\mathbf{T}\|_1 = \lambda + \min_{\mathbf{T} \in \Pi(\mathbf{a}, \mathbf{b})} G(\mathbf{T}).$$

## B. Optimization

Unlike [28], [30], and [31] that solved their respective dual problems, we directly consider the primal problem and express (10) by the following equivalent problem:

$$\min_{\mathbf{T} \in \Omega^1, \mathbf{U} \in \Omega^2, \mathbf{V} \in \Omega^3, \mathbf{W} \in \Omega^4} G(\mathbf{T}), \text{ s.t. } \mathbf{T} = \mathbf{U} = \mathbf{V} = \mathbf{W}, \quad (11)$$

where

$$\begin{aligned} \Omega^1 &= \{\mathbf{T} \in \mathbb{R}_+^{m \times n} \mid \mathbf{T}\mathbf{1}^n = \mathbf{a}\}, \\ \Omega^2 &= \{\mathbf{U} \in \mathbb{R}_+^{m \times n} \mid \mathbf{U}^\top \mathbf{1}^m = \mathbf{b}\}, \\ \Omega^3 &= \{\mathbf{V} \in \mathbb{R}_+^{m \times n} \mid \|\mathbf{V}[i, :]\|_0 \leq \rho^s \text{ for all } i \in \llbracket m \rrbracket\}, \\ \Omega^4 &= \{\mathbf{W} \in \mathbb{R}_+^{m \times n} \mid \|\mathbf{W}[:, i']\|_0 \leq \rho^t \text{ for all } i' \in \llbracket n \rrbracket\}. \end{aligned}$$

As we shall see shortly, such a constraint decomposition allows closed-form updates of all projection steps, whereas dual optimization does not admit an analytical solution in general. For example, we need to resort to solving a quadratic regularized OT problem that does not enjoy a closed-form solution unless  $\Pi(\mathbf{a}, \mathbf{b})$  is decomposed into the two constraint sets  $\Omega^1$  and  $\Omega^2$ .

After the reformulation (11), a penalty algorithm is applied. In particular, we consider a sequence of penalty subproblems, with the  $k$ -th subproblem given by

$$\min_{\mathbf{T} \in \Omega^1, \mathbf{U} \in \Omega^2, \mathbf{V} \in \Omega^3, \mathbf{W} \in \Omega^4} J_{\sigma^{(k)}}(\mathbf{T}, \mathbf{U}, \mathbf{V}, \mathbf{W}),$$

where

$$\begin{aligned} J_{\sigma^{(k)}}(\mathbf{T}, \mathbf{U}, \mathbf{V}, \mathbf{W}) &:= G(\mathbf{T}) + \frac{\sigma^{(k)}}{2} \|\mathbf{T} - \mathbf{U}\|_F^2 \\ &\quad + \frac{\sigma^{(k)}}{2} \|\mathbf{T} - \mathbf{V}\|_F^2 + \frac{\sigma^{(k)}}{2} \|\mathbf{T} - \mathbf{W}\|_F^2, \end{aligned}$$

which is solved approximately by updating the four variables alternately. Such an approach is summarized in Algorithm 1, which involves an outer loop and an inner loop. We use the index  $k$  for the outer iteration and  $l$  for the inner iteration. Each outer iteration corresponds to a subproblem, and the details of inner iterations are described as follows.

**Updating  $\mathbf{T}$ .** In each iteration  $l$ ,  $\mathbf{T}^{(k,l)}$  is updated via the projected gradient descent with fixed  $\mathbf{U}^{(k,l)}$ ,  $\mathbf{V}^{(k,l)}$ , and  $\mathbf{W}^{(k,l)}$  as follows:

$$\mathbf{T}^{(k,l+1)} = \text{proj}_{\Omega^1} \left( \mathbf{T}^{(k,l)} - \eta \mathbf{D}^{(k,l)} \right), \quad (12)$$

where  $\eta$  is the step-size and  $\mathbf{D}^{(k,l)}$  is the element-wise partial derivative of  $J_{\sigma^{(k)}}(\cdot)$  w.r.t.  $\mathbf{T}^{(k,l)}$ :

$$\mathbf{D}^{(k,l)} = \frac{\partial J_{\sigma^{(k)}}(\mathbf{T}^{(k,l)}, \mathbf{U}^{(k,l)}, \mathbf{V}^{(k,l)}, \mathbf{W}^{(k,l)})}{\partial \mathbf{T}}.$$

Instead of manually setting the step-size, the step-size  $\eta$  is found via the Armijo line search, which is crucial to guarantee the monotone decrease of  $J_{\sigma^{(k)}}(\cdot)$ . The projection operation after the gradient descent projects each row  $i$  of  $\mathbf{T}^{(k,l)} - \eta \mathbf{D}^{(k,l)}$  onto a ‘‘scaled’’ simplex  $\mathcal{A}_i = \{a_i \mathbf{x} \mid \mathbf{x} \in \Delta^n\}$ , which requires  $\mathcal{O}(mn \log n)$  time to find the closed-form solution (for further details about projecting a vector onto a simplex, see [59]). The per-iteration complexity for updating  $\mathbf{T}$  is thus  $\mathcal{O}(mn \log n)$ .

**Updating  $\mathbf{U}$ ,  $\mathbf{V}$ , and  $\mathbf{W}$ .** By the form of  $J_{\sigma^{(k)}}(\cdot)$ , the updates of  $\mathbf{U}$ ,  $\mathbf{V}$ , and  $\mathbf{W}$  can be conducted independently:

$$\min_{\mathbf{U} \in \Omega^2, \mathbf{V} \in \Omega^3, \mathbf{W} \in \Omega^4} J_{\sigma^{(k)}}(\mathbf{T}^{(k,l+1)}, \mathbf{U}, \mathbf{V}, \mathbf{W}), \quad (13)$$

which essentially projects  $\mathbf{T}^{(k,l+1)}$  onto  $\Omega^2$ ,  $\Omega^3$ , and  $\Omega^4$ , respectively.  $\mathbf{U}^{(k,l+1)}$  is obtained by projecting each column  $i'$  of  $\mathbf{T}^{(k,l+1)}$  onto a scaled simplex  $\mathcal{B}_{i'} = \{b_{i'} \mathbf{x} \mid \mathbf{x} \in \Delta^m\}$ , which incurs cost  $\mathcal{O}(mn \log m)$ . Despite the non-convexity of  $\Omega^3$  (resp.  $\Omega^4$ ),  $\mathbf{V}^{(k,l+1)}$  (resp.  $\mathbf{W}^{(k,l+1)}$ ) can be determined by finding the top- $\rho^s$  (resp.  $\rho^t$ ) entries of each row (resp. column) of  $\mathbf{T}^{(k,l+1)}$ , which involves per-iteration complexity  $\mathcal{O}(mn \log \rho^s)$  (resp.  $\mathcal{O}(mn \log \rho^t)$ ) [31]. Overall, the per-iteration complexity for updating the four variables is  $\mathcal{O}(mn \log \max\{m, n\})$ .

**Remark.** SCOTM can also be generalized to accommodate different matching budgets for different points, mutatis mutandis. For this variant, the optimization procedure remains valid since closed-form updates are still applicable, and the theorems have analogous versions, although the proofs will be lengthier. For succinctness, we have focused on the setting where all points in  $\mathcal{S}$  (resp.  $\mathcal{T}$ ) have the same matching budget.

**Convergence analysis.** To present the convergence guarantee of Algorithm 1, we define the following first-order optimality condition of (10), which is adapted from [60] and [61] to accommodate the constraints in our problem.

**Definition III.4.**  $\hat{\mathbf{T}}$  satisfies the *first-order optimality condition* of (10) if  $\hat{\mathbf{T}} \in \Omega_{\rho^s, \rho^t}$  and  $\sum_{ii'} \frac{\partial G(\hat{\mathbf{T}})}{\partial T_{ii'}} (T'_{ii'} - \hat{T}_{ii'}) \geq 0$  for all  $\mathbf{T}' \in \Pi(\mathbf{a}, \mathbf{b}) \cap \Omega_{\rho^s, \rho^t}$ .

Based on the first-order optimality condition, the following theorem gives a theoretical guarantee of Algorithm 1.

**Theorem III.5.** *Algorithm 1 satisfies:*

- 1) For each outer iteration  $k \geq 0$ , Algorithm 1 generates  $(\mathbf{T}^{(k+1)}, \mathbf{U}^{(k+1)}, \mathbf{V}^{(k+1)}, \mathbf{W}^{(k+1)})$  in a finite number of inner iterations;
- 2) The sequence  $\{\mathbf{T}^{(k)}, \mathbf{U}^{(k)}, \mathbf{V}^{(k)}, \mathbf{W}^{(k)}\}_k$  admits a limit point  $(\hat{\mathbf{T}}, \hat{\mathbf{U}}, \hat{\mathbf{V}}, \hat{\mathbf{W}})$ ;
- 3) Every limit point satisfies that  $\hat{\mathbf{T}} = \hat{\mathbf{U}} = \hat{\mathbf{V}} = \hat{\mathbf{W}}$  and  $\hat{\mathbf{T}}$  is a first-order optimal solution.

Theorem III.5 demonstrates that Algorithm 1 is well-defined, and the sequence generated by it admits a limit point that satisfies the first-order optimality condition. In practice, Algorithm 1 can be terminated when  $\mathbf{T}^{(k)}$ ,  $\mathbf{U}^{(k)}$ ,  $\mathbf{V}^{(k)}$ , and  $\mathbf{W}^{(k)}$  are sufficiently close to each other.

## IV. EXPERIMENTS

In this section, we empirically verify the effectiveness of SCOTM on various tasks. In all tasks, the outer loops are terminated when

$$\sqrt{\|\mathbf{T}^{(k)} - \mathbf{U}^{(k)}\|_F^2 + \|\mathbf{T}^{(k)} - \mathbf{V}^{(k)}\|_F^2 + \|\mathbf{T}^{(k)} - \mathbf{W}^{(k)}\|_F^2} \leq 10^{-4}.$$

Throughout this section, we choose  $\sigma^{(0)} = 10$ ,  $\theta = 2.0$ , and  $\epsilon^{(k)} = 0.99^k \times 10^{-4}$  for hyperparameters in Algorithm 1, unless specified otherwise. The experiments are conducted on a Ubuntu 18.04 server with two 28-core 2.40 GHz Intel®

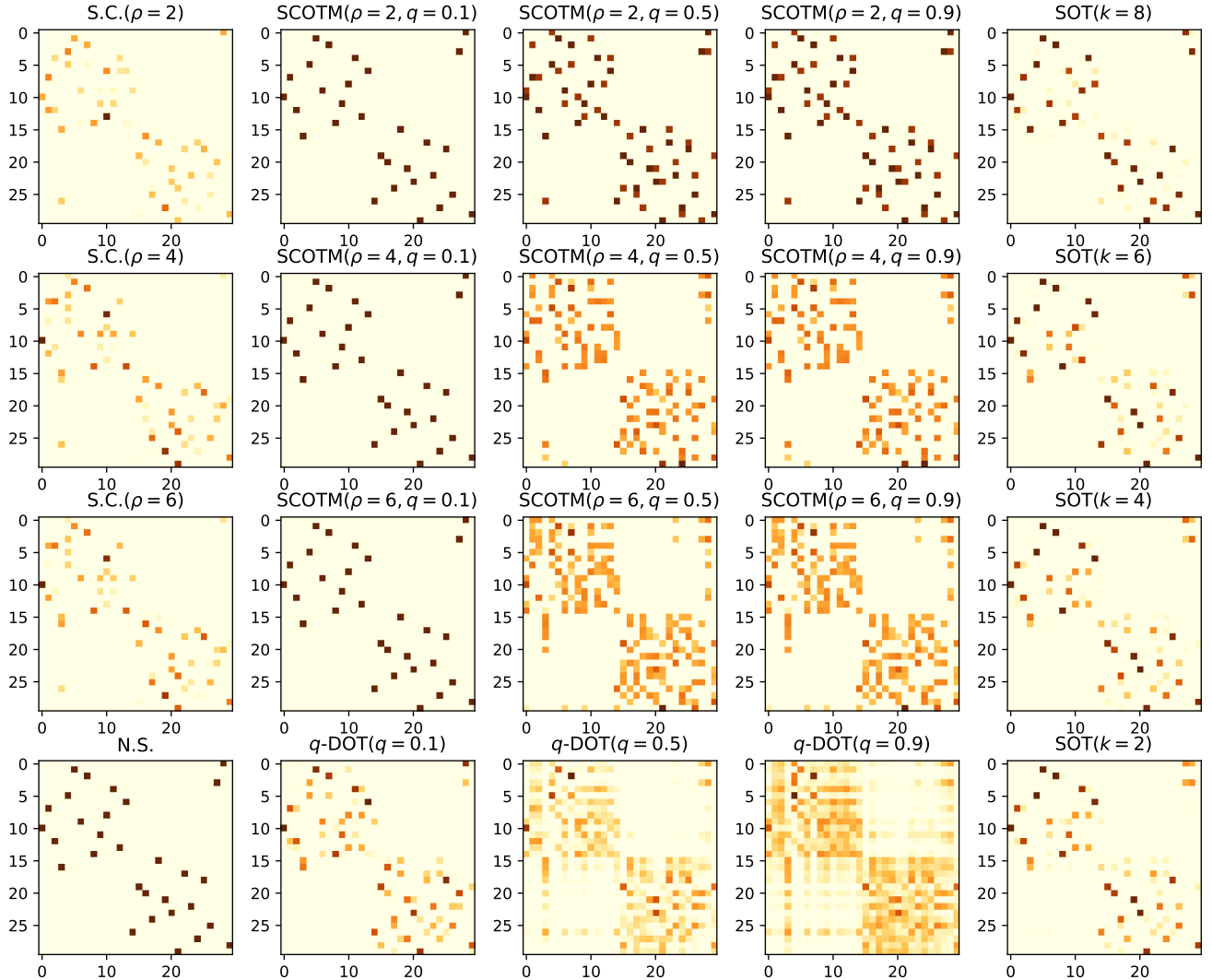


Fig. 3: A comparison of the transport plans obtained by the network simplex solver (N.S.), sparsity-constrained OT (S.C.),  $q$ -regularized OT ( $q$ -DOT), structured OT (SOT), and SCOTM. The darker the color is, the larger the value of the corresponding entry is in the transport plan.

TABLE I: The percentage of non-zero entries in the transport plans obtained by the network simplex solver of OT (N.S.), sparsity-constrained OT (S.C.),  $q$ -regularized OT ( $q$ -DOT), structured OT (SOT), and SCOTM.

N.S.	SOT				$q$ -DOT			S.C.			SCOTM								
	$k=8$	$k=6$	$k=4$	$k=2$	$q=.1$	$q=.5$	$q=.9$	$\rho=2$	$\rho=4$	$\rho=6$	$\rho=2$			$\rho=4$			$\rho=6$		
											$q=.1$	$q=.5$	$q=.9$	$q=.1$	$q=.5$	$q=.9$	$q=.1$	$q=.5$	$q=.9$
3.3	57.1	59.4	73.4	82.9	8.8	33.2	98.9	5.9	6.3	6.3	4.8	6.7	6.7	7.4	13.2	13.3	7.5	19.4	20.0

Xeon® E5-2680 v4 CPUs and 378 GB of RAM. The source code is written in Python 3.6 and is included in the supplementary material. The package dependencies are listed in the requirements.txt file in the code submission.

#### A. Matching Synthetic Point Clouds

**Experimental setup.** In the first set of experiments, we seek to understand the characteristics of transport plans obtained by SCOTM. We synthesize two point clouds in  $\mathbb{R}^2$  from the two-Gaussian mixture  $0.5\mathcal{N}(\begin{bmatrix} 0 \\ 0 \end{bmatrix}, \begin{bmatrix} 1 & 0 \\ 0 & 1 \end{bmatrix}) + 0.5\mathcal{N}(\begin{bmatrix} 2 \\ 2 \end{bmatrix}, \begin{bmatrix} 1 & 0 \\ 0 & 1 \end{bmatrix})$ . Both point clouds contain 30 points. The cost function  $c(\cdot, \cdot)$  is fixed

to the squared Euclidean distance. Both the source and target distributions are uniform.

**Baselines.** The baselines include the network simplex solver for OT [48], sparsity-constrained OT [31],  $q$ -regularized OT [30], and structured OT [55] that divides support points into subregions and encourages correlations of the matching within the same subregion. For structured OT, we used  $k$ -means clustering to obtain subregions. We used the same value  $\rho$  for both  $\rho^s$  and  $\rho^t$ , and tested different values of  $\rho$  for SCOTM. The regularization weight,  $\gamma = 0.1$ , was shared by sparsity-constrained OT,  $q$ -regularized OT, and SCOTM.

**Sparsity.** The transport plans obtained by different methods

TABLE II: The performance of many-to-many matching methods in student course allocation with various  $\rho^s$ .

	$\rho^s = 10$			$\rho^s = 20$			$\rho^s = 40$		
	SCOTM	KMB	LBF	SCOTM	KMB	LBF	SCOTM	KMB	LBF
top-1 (%)	<b>22.1</b>	20.8	11.8	<b>32.7</b>	<b>32.7</b>	12.6	<b>49.3</b>	<b>49.3</b>	17.7
top-5 (%)	<b>62.3</b>	52.0	40.3	<b>81.1</b>	75.7	39.7	<b>93.9</b>	92.8	66.0
Runtime (sec.)	<b>12.2</b>	247.6	400.5	<b>12.8</b>	943.4	1452.8	<b>12.9</b>	6259.8	7599.6

TABLE III: The performance of SCOTM in student course allocation with various values of  $q$ .

$q$	0	0.1	0.5	0.8	0.9	0.99	0.999
top-1 (%)	<b>32.7</b>						
top-5 (%)	65.4	66.2	76.8	76.8	<b>81.1</b>	<b>81.1</b>	<b>81.1</b>

TABLE IV: The performance of SCOTM in student course allocation with various values of  $\gamma$ .

$\gamma$	0.01	0.02	0.05	0.1	0.2	0.5	1	2	5	10
top-1 (%)	<b>32.7</b>	30.5	30.0	29.8						
top-5 (%)	73.7	76.8	<b>81.1</b>	<b>81.1</b>	<b>81.1</b>	<b>81.1</b>	<b>81.1</b>	75.7	74.1	73.7

TABLE V: Runtime (sec.) of SCOTM in student course allocation with varying  $\sigma^{(0)}$ ,  $\theta$ , and  $\epsilon^{(k)}$ .

$\sigma^{(0)}$	$\theta$	1			10			100		
		1.2	2.0	2.5	1.2	2.0	2.5	1.2	2.0	2.5
Bases of $\epsilon^{(k)}$	<b>0.999</b>	27.1	14.1	<b>11.4</b>	25.4	12.4	<b>10.3</b>	8.6	4.5	<b>4.1</b>
	<b>0.99</b>	28.7	14.1	11.5	25.6	12.8	10.4	8.8	4.6	4.1
	<b>0.9</b>	78.3	15.4	11.5	44.6	12.8	10.6	9.9	5.0	4.2
	<b>0.8</b>	395.4	31.2	13.3	103.3	15.0	10.7	37.0	5.2	4.6

TABLE VI: PINs of C.elegans (CE), D.melanogaster (DM), H.sapiens (HS), M.musculus (MM), and S.cerevisiae (SC).

PINs	CE	DM	HS	MM	SC
# nodes	19,756	14,098	22,369	24,855	6,659
# edges	4,884	25,054	55,168	592	82,932

are visualized in Figure 3 and the corresponding non-zero entry percentages are reported in Table I. The transport plan obtained by the network simplex solver is maximally sparse. For sparsity-constrained OT and  $q$ -regularized OT, the transport plan becomes denser with  $\rho$  and  $q$  increasing, respectively. The transport plan of structured OT becomes sparser as  $k$  increases because fewer transport plan entries are correlated, however, it is hard to directly control the sparsity. SCOTM obtains sparser transport plans than  $q$ -regularized OT with the same  $q$  especially when  $q$  is relatively large. Owing to the adoption of the deformed  $q$ -entropy regularization, SCOTM outputs denser transport plans than sparsity-constrained OT when  $\rho = 4$  or  $\rho = 6$ . Figure 3 and Table I showcase that SCOTM can control the sparsity of transport plans directly and flexibly. Specifically, while SCOTM uses parameters  $q$ ,  $\rho^s$ , and  $\rho^t$  to control the sparsity of transport plans, practitioners can simply set  $q$  close to 1, and adjust matching budget constraints  $\rho^s$  and  $\rho^t$  to achieve the required sparsity and thus the desired number of matched pairs. Such a property is essential to extract interpretable many-to-many matching and cannot be achieved by naive OT or its existing variants. This unique property makes SCOTM user-friendly.

### B. Student Course Allocation

**Experimental setup.** We proceed to consider the student course allocation problem using the real-world Harvard course allocation dataset [62]. This dataset, obtained through a survey,

comprises the preference rankings of 456 students for 96 courses. The preference score for each student's  $k^{\text{th}}$  favorite course is assigned as  $\frac{1}{k}$  and the corresponding matching cost is  $1 - \frac{1}{k}$ . We compared SCOTM with  $q = 0.9$  and  $\gamma = 0.1$ , against state-of-the-art many-to-many matching algorithms, including KMB [32] and LBF [33]. The performance for different values of  $q$  and  $\gamma$  is discussed in the appendix. Assuming that each student can select at most  $\rho^t = 5$  courses, we evaluate the percentage of  $k^{\text{th}}$  favorite courses being selected (referred to as top- $k$ ) and the runtime of these methods for various  $\rho^s$  values.

**Results in student course allocation.** As demonstrated in Table II, SCOTM exhibits superior computational efficiency compared to KMB and LBF. For instance, when each course permits at most 40 students, SCOTM's runtime is 99.79% and 99.83% less than that of KMB and LBF, respectively. On both the top-1 and top-5 metrics, SCOTM achieves performance that is similar to or better than KMB and LBF. To further understand the performance of SCOTM on the student course allocation task, we conduct sensitivity analyses of  $q$ ,  $\gamma$ ,  $\sigma^{(0)}$ ,  $\theta$ , and  $\epsilon^{(k)}$  while fixing  $\rho^s = 20$  and  $\rho^t = 5$ .

**Sensitivity analysis of  $q$ .** As is demonstrated in Table III, when  $q \geq 0.9$ , SCOTM is not sensitive to the choice of  $q$ . When  $q$  is too small, the transport plan is likely to be too sparse and the top-5 metric tends to decrease, which justifies our usage of deformed  $q$ -entropy to promote matches.

**Influence of  $\gamma$ .** We further study the impact of the regularization weight  $\gamma$  by fixing  $q = 0.9$  and varying values of  $\gamma$ . As is shown in Table IV, SCOTM is insensitive to  $\gamma$  and achieves the best performance when  $\gamma \in [0.05, 1]$ . When  $\gamma$  gets too small, top-5 decreases but top-1 does not, which is due to the fact that the transport plan becomes sparse. On the other hand, if  $\gamma$  is too large, both top-1 and top-5 deteriorate as the matching costs contribute insufficiently.

TABLE VII: Recall, Precision, and F1 (in percent) of various methods in PIN matching experiment.

Methods	CE→SC			CE→DM			HS→MM		
	Recall	Precision	F1	Recall	Precision	F1	Recall	Precision	F1
<b>PrimAlign</b>	1.1	<b>62.7</b>	2.2	5.8	<b>86.7</b>	10.9	0.9	<b>42.6</b>	1.7
<b>NetCoffee2</b>	3.9	5.2	4.4	2.4	3.2	2.7	1.2	2.7	1.6
<b>N.S.</b>	0.3	43.9	0.5	0.3	45.6	0.5	0.1	24.5	0.2
<b>S.C.</b>	0.1	10.4	0.2	0.1	43.3	0.1	0.1	11.8	0.1
<b><i>q</i>-DOT</b>	<b>100.0</b>	5.3	10.1	<b>100.0</b>	3.2	6.2	<b>100.0</b>	2.7	5.3
<b>SCOTM</b>	45.1	31.1	<b>36.8</b>	47.3	32.2	<b>38.3</b>	23.7	27.2	<b>25.3</b>

TABLE VIII: Runtime (in sec.) of various methods in PIN matching experiment.

Methods	PrimAlign	NetCoffee2	N.S.	S.C.	<i>q</i> -DOT	SCOTM
<b>CE→SC</b>	1762.3	3346.0	6.9	1934.3	287.7	1079.2
<b>CE→DM</b>	14807.8	13288.1	33.9	8744.0	3211.2	2878.0
<b>HS→MM</b>	107916.0	64736.9	1351.2	20347.9	11314.3	17703.2

TABLE IX: Recall, Precision, and F1 (in percent) of SCOTM with various  $\rho$ 's in PIN matching experiment.

$\rho$	32	64	128	256	512	1024
Recall	0.9	2.6	7.7	25.9	45.1	<b>69.5</b>
Precision	9.7	7.1	<b>42.5</b>	35.9	31.1	24.0
F1	1.6	3.8	13.3	30.1	<b>36.8</b>	35.7

TABLE X: Recognition rate (in percent) of as a function of increasing perturbation in feature matching-based object recognition experiment. Methods include Network Simplex solver of OT (N.S.), sparsity-constrained OT (S.C.), *q*-regularized OT (*q*-DOT), and SCOTM.

Perturbation	0%	10%	20%	30%
<b>N.S.</b>	85.2	81.1	73.7	67.7
<b>S.C.</b>	87.4	81.5	77.8	70.3
<b><i>q</i>-DOT</b>	44.4	38.3	33.3	30.9
<b>SCOTM</b>	<b>87.7</b>	<b>85.2</b>	<b>81.5</b>	<b>79.0</b>

**Influence of  $\sigma^{(0)}$ ,  $\theta$ , and  $\epsilon^{(k)}$ .** To understand the roles of  $\sigma^{(0)}$ ,  $\theta$ , and  $\epsilon^{(k)}$ , We run SCOTM with  $\sigma^{(0)} \in \{1, 10, 100\}$ ,  $\theta \in \{1.2, 2.0, 2.5\}$ , and  $\epsilon^{(k)} \in 10^{-4} \times \{0.999^k, 0.99^k, 0.9^k, 0.8^k\}$ . Table V demonstrates that larger  $\sigma^{(0)}$  and  $\theta$  and larger bases of  $\epsilon^{(k)}$  tend to reduce time. However, the matching quality is not sensitive to them since all cases yield top-5 values between 80.3% and 81.1% and top-1 remains a constant 32.7%.

### C. Matching Protein Interaction Networks

**Experimental setup.** Five extensively studied species are considered [63]–[65], including *C.elegans* (worm), *D.melanogaster* (fly), *H.sapiens* (human), *M.musculus* (mouse), and *S.cerevisiae* (yeast).<sup>2</sup> Table VI summarizes the statistics of these datasets. We evaluate the performance of various methods using the hierarchical Gene Ontology (GO) categorization, where proteins are annotated with appropriate GO categories organized as a directed acyclic graph. As is the common practice in the literature [42], [64], we restrict the protein annotations to level five of the GO directed acyclic graph. A protein pair that shares at least one annotation is considered as a true match. The sequence similarity of proteins is used to set the corresponding matching cost. We

<sup>2</sup>These datasets can be downloaded from <http://webprs.khas.edu.tr/~cesim/BEAMS.tar.gz>.

TABLE XI: Recognition rate (in percent) of SCOTM with varying values of  $\rho$  and  $\gamma$  when the perturbation is 30%.

$\rho \backslash \gamma$	0.01	0.02	0.05	0.1	0.2
<b>4</b>	79.0	79.0	77.9	77.9	76.6
<b>8</b>	79.0	79.0	79.0	77.9	76.6
<b>16</b>	79.0	79.0	79.0	77.6	75.3

compare SCOTM against other OT-based methods and state-of-the-art many-to-many graph matching methods including PrimAlign [9] and NetCoffee2 [65]. For *q*-regularized OT and SCOTM, we chose  $q = 0.9$ . We set regularization weight  $\gamma = 0.1$  and used the same value  $\rho$  for both  $\rho^s$  and  $\rho^t$ .

**Results in matching protein interaction networks.** Table VII reports the results when  $\rho = 512$ . SCOTM achieves a good balance between recall and precision, and outperforms baselines by a large margin in terms of F1. Both the network simplex solver and sparsity-constrained OT exhibit low recall values because their transport plans are overly sparse. In contrast, the transport plans of *q*-regularized OT are overly dense. Table VII summarizes the runtime of various methods. SCOTM has similar runtime to sparsity-constrained OT and *q*-regularized OT, and has higher computational efficiency than PrimAlign and NetCoffee2. We further compared the performance of SCOTM with various  $\rho$ 's, which is reported in Table IX. Increasing  $\rho$  can increase recall since SCOTM outputs more matched pairs. On the other hand, the precision may decrease when  $\rho$  is too large.

### D. Object Recognition

**Experimental setup.** In this subsection, we conduct a shape retrieval experiment on the benchmark COIL-20 dataset that includes 20 objects with 72 views each. Following [22], we begin by removing 36 (of the 72) representative views of each object (every other view), and use these removed views as queries to the remaining view database (the other 36 views for each of the 20 objects). Each object's silhouette is then represented by a discrete skeleton, i.e., a set of points supported on two-dimensional Euclidean spaces. We then perform PCA-based alignment for obtained points and compute the discrepancies between each "query" view and each of the remaining database views according to the optimized objectives of optimal transport and its variants. For

TABLE XII: Empirical results on prioritized task assignment.

n	metrics	KMB	LBF	SCOTM (h = 8)	SCOTM (h = 7)	SCOTM (h = 6)
32	PPPM (%)	8.8	11.3	<b>23.7</b>	20.6	15.7
	PSMBPP (%)	51.9	66.7	<b>100.0</b>	<b>100.0</b>	88.9
	Runtime (sec.)	1.5	22.1	1.0	0.9	0.8
128	PPPM (%)	9.5	8.4	<b>24.8</b>	21.2	16.9
	PSMBPP (%)	52.1	46.2	<b>99.2</b>	96.6	92.3
	Runtime (sec.)	131.4	350.1	1.9	1.6	1.8
512	PPPM (%)	9.8	9.1	<b>29.1</b>	17.0	16.5
	PSMBPP (%)	54.5	50.8	<b>100.0</b>	94.8	91.9
	Runtime (sec.)	29355.4	11919.9	27.6	26.1	25.2

any given query view, we predict its object using the object of the database view that has the smallest discrepancy. We use the same  $\rho = 8$  value for both  $\rho^s$  and  $\rho^t$ . The regularization weight  $\gamma = 0.01$  is shared by all OT variants. We set  $q = 0.9$  for both  $q$ -regularized OT and SCOTM. To also perform perturbation studies, we randomly remove 10%, 20%, and 30% of points.

**Results in object recognition.** The detailed experimental results are reported in Table X. Our method achieves the best performance and is more robust to the perturbation than baselines. Furthermore, the sensitivity analysis in Table XI demonstrates that our method is insensitive to the choice of  $\rho$  and  $\gamma$ .

### E. Prioritized Task Assignment

**Experimental setup.** Next, we verify the effectiveness of SCOTM for prioritized matching on a group of synthetic datasets. In this group of datasets, the cardinalities of  $\mathcal{S}$  and  $\mathcal{T}$  are equal, i.e.,  $m = n$ . We compare SCOTM with state-of-the-art many-to-many matching methods, including KMB [32] and LBF [33], when  $n$  is set to 32, 128, and 512, respectively. The matching budget constraints are given by  $\rho^s = 9$  and  $\rho^t = 5$ , that is, each task can be assigned to at most 9 agents and each agent can undertake at most 5 tasks. We randomly set  $r = 10\%$  of the points in  $\mathcal{S}$  as prioritized points. The cost of matching  $s_i$  to  $t_{i'}$  follows a uniform distribution from 0 to 1. Given a matching matrix  $\mathbf{T} = [T_{ii'}]$ , we evaluate the Proportion of Prioritized Points' Matches out of all matches (PPPM), as well as the Proportion of Satisfied Matching Budgets for Prioritized Points (PSMBPP), defined as follows:

$$\text{PPPM}(\mathbf{T}) = \frac{|\{(i, i') \mid T_{ii'} \neq 0 \text{ and } i \text{ is a prioritized point}\}|}{|\{(i, i') \mid T_{ii'} \neq 0\}|},$$

$$\text{PSMBPP}(\mathbf{T}) = \frac{|\{(i, i') \mid T_{ii'} \neq 0 \text{ and } i \text{ is a prioritized point}\}|}{\rho^s m r}.$$

In SCOTM,  $\mathbf{a}$  is set according to Eq. (8), and  $\mathbf{b}$  is set as a uniform distribution. It is easy to verify that (9) holds for all  $h \in \llbracket \rho^s - 1 \rrbracket$ .

**Results in prioritized task assignment.** The experimental results are reported in Table XII. The PPPM values of KMB and LBF is close to 10%, which implies that they treat all points equally. SCOTM achieves higher PPPM and PSMBPP values than KMB and LBF, which verifies that SCOTM can perform prioritized matching. One can also observe that SCOTM always has PSMBPP higher than  $\frac{h}{\rho^s}$ , which is consistent with Theorem III.2. SCOTM is also orders of magnitude faster than KMB and LBF.

### CONCLUSION

In this paper, we proposed a practical OT-based many-to-many matching method based on two components: the  $\ell_0$  constraints (matching budget) on each row and column in a transport plan, and the recently-proposed deformed  $q$ -entropy regularization. The former sparsifies a matching, while the latter encourages a point to maximally meet the matching budget constraints. A theoretically guaranteed algorithm was then derived to determine a transport plan effectively and efficiently. Experimental results on various tasks demonstrate the proposed method successfully extracts many-to-many matchings and achieves good performance.

### REFERENCES

- [1] H. Li, J. Xu *et al.*, "Semantic matching in search," *Foundations and Trends® in Information Retrieval*, vol. 7, no. 5, pp. 343–469, 2014.
- [2] C. Xu, J. Xu, Z. Dong, and J.-R. Wen, "Syntactic-informed graph networks for sentence matching," *ACM Transactions on Information Systems*, vol. 42, no. 2, pp. 1–29, 2023.
- [3] H. Xu, Q. Peng, H. Liu, Y. Sun, and W. Wang, "Group-based personalized news recommendation with long-and short-term fine-grained matching," *ACM Transactions on Information Systems*, 2023.
- [4] J. Colannino, M. Damian, F. Hurtado, S. Langerman, H. Meijer, S. Ramaswami, D. Souvaine, and G. Toussaint, "Efficient many-to-many point matching in one dimension," *Graphs and Combinatorics*, vol. 23, no. 1, pp. 169–178, 2007.
- [5] F. Rajabi-Alni and A. Bagheri, "Limited-capacity many-to-many point matching in one dimension," *arXiv preprint arXiv:1210.8123*, 2012.
- [6] —, "A faster algorithm for the limited-capacity many-to-many point matching in one dimension," *arXiv preprint arXiv:1904.03015*, 2019.
- [7] G. T. Toussaint *et al.*, "A comparison of rhythmic similarity measures," in *International Society for Music Information Retrieval*, 2004.
- [8] L. Sun, Y. Manabe, and N. Yata, "Sparse group match for point cloud registration," *ITE Transactions on Media Technology and Applications*, vol. 6, no. 2, pp. 151–161, 2018.
- [9] K. Kalecky and Y.-R. Cho, "PrimAlign: Pagerank-inspired markovian alignment for large biological networks," *Bioinformatics*, vol. 34, no. 13, pp. i537–i546, 2018.
- [10] Y. Tan, C. Y. Member, X. Wei, Z. Wu, and X. Zheng, "Partial relaxed optimal transport for denoised recommendation," *arXiv preprint arXiv:2204.08619*, 2022.
- [11] C. Villani, *Optimal Transport: Old and New*. Springer Science & Business Media, 2008, vol. 338.
- [12] G. Monge, "Mémoire sur la theorie des deblais et des remblais histoire de l'académie royale des sciences," in *Année MDCCLXXXI, avec les Mémoires de Mathématique et de Physique, pour la meme Année*. Tirés des Registres de cette Académie Paris, 1781, pp. 666–704.
- [13] L. V. Kantorovich, "Mathematical methods of organizing and planning production," *Management Science*, vol. 6, no. 4, pp. 366–422, 1960.
- [14] H.-T. Yu, A. Jatowt, H. Joho, J. M. Jose, X. Yang, and L. Chen, "Wassrank: Listwise document ranking using optimal transport theory," in *Proceedings of the twelfth ACM international conference on web search and data mining*, 2019, pp. 24–32.
- [15] M. Cuturi, O. Teboul, and J.-P. Vert, "Differentiable ranking and sorting using optimal transport," *Advances in neural information processing systems*, vol. 32, 2019.

- [16] H. Xu, D. Luo, H. Zha, and L. C. Duke, "Gromov-Wasserstein learning for graph matching and node embedding," in *International Conference on Machine Learning*, 2019.
- [17] H. P. Maretic, M. El Gheche, G. Chierchia, and P. Frossard, "GOT: an optimal transport framework for graph comparison," in *Advances in Neural Information Processing Systems*, 2019.
- [18] Z. Huang, P. Yu, and J. Allan, "Improving cross-lingual information retrieval on low-resource languages via optimal transport distillation," in *Proceedings of the Sixteenth ACM International Conference on Web Search and Data Mining*, 2023, pp. 1048–1056.
- [19] N. Hu, X. Huang, W. Li, X. Li, and A.-A. Liu, "Cross-domain image-object retrieval based on weighted optimal transport," *IEEE Transactions on Multimedia*, 2023.
- [20] C. Villani, "The Wasserstein distances," *Optimal Transport: Old and New*, pp. 93–111, 2009.
- [21] Y. Keselman, A. Shokoufandeh, M. F. Demirci, and S. Dickinson, "Many-to-many graph matching via metric embedding," in *IEEE / CVF Computer Vision and Pattern Recognition Conference.*, vol. 1. IEEE, 2003, pp. 1–1.
- [22] M. F. Demirci, A. Shokoufandeh, Y. Keselman, L. Bretzner, and S. Dickinson, "Object recognition as many-to-many feature matching," *International Journal of Computer Vision*, vol. 69, no. 2, pp. 203–222, 2006.
- [23] M. F. Demirci and Y. Osmanloğlu, "Many-to-many matching under the  $\ell_1$  norm," in *International Conference on Image Analysis and Processing*. Springer, 2009, pp. 787–796.
- [24] M. F. Demirci, Y. Osmanloğlu, A. Shokoufandeh, and S. Dickinson, "Efficient many-to-many feature matching under the  $\ell_1$  norm," *Computer Vision and Image Understanding*, vol. 115, no. 7, pp. 976–983, 2011.
- [25] R. A. Brualdi, *Combinatorial Matrix Classes*. Cambridge University Press, 2006, vol. 13.
- [26] G. Peyre and M. Cuturi, "Computational optimal transport," *arXiv: Machine Learning*, 2018.
- [27] M. Cuturi, "Sinkhorn distances: Lightspeed computation of optimal transport," in *Advances in Neural Information Processing Systems*, 2013, pp. 2292–2300.
- [28] M. Blondel, V. Seguy, and A. Rolet, "Smooth and sparse optimal transport," in *International Conference on Artificial Intelligence and Statistics*. PMLR, 2018, pp. 880–889.
- [29] Y. Xie, X. Wang, R. Wang, and H. Zha, "A fast proximal point method for computing exact wasserstein distance," in *Uncertainty in Artificial Intelligence*. PMLR, 2020, pp. 433–453.
- [30] H. Bao and S. Sakaue, "Sparse regularized optimal transport with deformed q-entropy," *Entropy*, vol. 24, no. 11, p. 1634, 2022.
- [31] T. Liu, J. Puigcerver, and M. Blondel, "Sparsity-constrained optimal transport," in *The Eleventh International Conference on Learning Representations*, 2023.
- [32] H. Zhu, D. Liu, S. Zhang, Y. Zhu, L. Teng, and S. Teng, "Solving the many to many assignment problem by improving the kuhn–munkres algorithm with backtracking," *Theoretical Computer Science*, vol. 618, pp. 30–41, 2016.
- [33] N. Das and P. A. Priya, "A gradient-based interior-point method to solve the many-to-many assignment problems," *Complexity*, vol. 2019, 2019.
- [34] K. Hamidouche, W. Saad, and M. Debbah, "Many-to-many matching games for proactive social-caching in wireless small cell networks," in *International Symposium on Modeling and Optimization in Mobile, Ad Hoc, and Wireless Networks (WiOpt)*. IEEE, 2014, pp. 569–574.
- [35] P. Biró and J. Gudmundsson, "Complexity of finding pareto-efficient allocations of highest welfare," *European Journal of Operational Research*, vol. 291, no. 2, pp. 614–628, 2021.
- [36] P. Xepapadeas, "Serial dictatorship vs. nash in assessing pareto optimality in many-to-many matchings with an application in water management," *Nash in Assessing Pareto Optimality in Many-to-Many Matchings With an Application in Water Management (October 14, 2022)*, 2022.
- [37] F. Echenique and J. Oviedo, "A theory of stability in many-to-many matching markets," 2004.
- [38] N. Chen and M. Li, "Pareto stability in two-sided many-to-many matching with weak preferences," *Journal of Mathematical Economics*, vol. 82, pp. 272–284, 2019.
- [39] M. Peski, "Tractable model of dynamic many-to-many matching," *American Economic Journal: Microeconomics*, vol. 14, no. 2, pp. 1–43, 2022.
- [40] K. Cechlárová, B. Klaus, and D. F. Manlove, "Pareto optimal matchings of students to courses in the presence of prerequisites," *Discrete Optimization*, vol. 29, pp. 174–195, 2018.
- [41] A. Utture, V. Somani, P. Krishnaa, and M. Nasre, "Student course allocation with constraints," in *International Symposium on Experimental Algorithms*. Springer, 2019, pp. 51–68.
- [42] R. Singh, J. Xu, and B. Berger, "Global alignment of multiple protein interaction networks with application to functional orthology detection," *Proceedings of the National Academy of Sciences*, vol. 105, no. 35, pp. 12 763–12 768, 2008.
- [43] K. Cechlárová, P. Eirinakis, T. Fleiner, D. Magos, I. Mourtos, and E. Potpinková, "Pareto optimality in many-to-many matching problems," *Discrete Optimization*, vol. 14, pp. 160–169, 2014.
- [44] K. Cechlárová, P. Eirinakis, T. Fleiner, D. Magos, D. Manlove, I. Mourtos, E. Oceláková, and B. Rastegari, "Pareto optimal matchings in many-to-many markets with ties," *Theory of Computing Systems*, vol. 59, pp. 700–721, 2016.
- [45] K. Bando, T. Hirai, and J. Zhang, "Substitutes and stability for many-to-many matching with contracts," *Games and Economic Behavior*, vol. 129, pp. 503–512, 2021.
- [46] F. Rajabi-Alni, "Two exact algorithms for the generalized assignment problem," *arXiv preprint arXiv:1303.4031*, 2013.
- [47] H. Zhu and M. Zhou, "M-M role-transfer problems and their solutions," vol. 39, no. 2, p. 448–459, mar 2009.
- [48] R. E. Tarjan, "Dynamic trees as search trees via euler tours, applied to the network simplex algorithm," *Mathematical Programming*, vol. 78, no. 2, pp. 169–177, 1997.
- [49] D. Ge, H. Wang, Z. Xiong, and Y. Ye, "Interior-point methods strike back: Solving the wasserstein barycenter problem," *Advances in Neural Information Processing Systems*, vol. 32, 2019.
- [50] M. Zaslavskiy, F. Bach, and J.-P. Vert, "Many-to-many graph matching: a continuous relaxation approach," in *Joint European Conference on Machine Learning and Knowledge Discovery in Databases*. Springer, 2010, pp. 515–530.
- [51] T. Iwata and K. Ishiguro, "Robust unsupervised cluster matching for network data," *Data Mining and Knowledge Discovery*, vol. 31, no. 4, pp. 1132–1154, 2017.
- [52] T. Iwata, T. Hirao, and N. Ueda, "Topic models for unsupervised cluster matching," *IEEE Transactions on Knowledge and Data Engineering*, vol. 30, no. 4, pp. 786–795, 2017.
- [53] M. Weylandt, G. Michailidis, and T. M. Roddenberry, "Sparse partial least squares for coarse noisy graph alignment," in *IEEE Statistical Signal Processing Workshop (SSP)*. IEEE, 2021, pp. 561–565.
- [54] J. Solomon, G. Peyré, V. G. Kim, and S. Sra, "Entropic metric alignment for correspondence problems," *ACM Transactions on Graphics (ToG)*, vol. 35, no. 4, pp. 1–13, 2016.
- [55] D. Alvarez-Melis, T. Jaakkola, and S. Jegelka, "Structured optimal transport," in *International Conference on Artificial Intelligence and Statistics*. PMLR, 2018, pp. 1771–1780.
- [56] C.-H. Lin, M. Azabou, and E. Dyer, "Making transport more robust and interpretable by moving data through a small number of anchor points," in *International Conference on Machine Learning*. PMLR, 2021, pp. 6631–6641.
- [57] Y. C. F. Lim, L. Wynter, and S. H. Lim, "Order constraints in optimal transport," in *International Conference on Machine Learning*. PMLR, 2022, pp. 13 313–13 333.
- [58] W. Rudin, *Principles of Mathematical Analysis*. McGraw-hill New York, 1976, vol. 3.
- [59] W. Wang and M. A. Carreira-Perpinán, "Projection onto the probability simplex: An efficient algorithm with a simple proof, and an application," *arXiv preprint arXiv:1309.1541*, 2013.
- [60] Z. Lu and Y. Zhang, "Sparse approximation via penalty decomposition methods," *SIAM Journal on Optimization*, vol. 23, no. 4, pp. 2448–2478, 2013.
- [61] M. Lapucci, T. Levato, and M. Sciandrone, "Convergent inexact penalty decomposition methods for cardinality-constrained problems," *Journal of Optimization Theory and Applications*, vol. 188, no. 2, pp. 473–496, 2021.
- [62] E. Budish and E. Cantillon, "The multi-unit assignment problem: Theory and evidence from course allocation at harvard," *American Economic Review*, vol. 102, no. 5, pp. 2237–2271, 2012.
- [63] S. M. E. Sahraeian and B.-J. Yoon, "Smetana: accurate and scalable algorithm for probabilistic alignment of large-scale biological networks," *PLoS one*, vol. 8, no. 7, p. e67995, 2013.
- [64] F. Alkan and C. Erten, "Beams: backbone extraction and merge strategy for the global many-to-many alignment of multiple ppi networks," *Bioinformatics*, vol. 30, no. 4, pp. 531–539, 2014.
- [65] J. Hu, J. He, J. Li, Y. Gao, Y. Zheng, and X. Shang, "A novel algorithm for alignment of multiple ppi networks based on simulated annealing," *BMC genomics*, vol. 20, no. 13, pp. 1–7, 2019.

- [66] D. P. Bertsekas, *Nonlinear Programming*, 2nd ed. Athena Scientific, 1999.